Energy Conversion and Management 195 (2019) 927–942

Contents lists available at ScienceDirect

Energy Conversion and Management

journal homepage: www.elsevier.com/locate/enconman

An opposition-based sine cosine approach with local search for parameter estimation of photovoltaic models

Huiling Chen[a], Shan Jiao[a], Ali Asghar Heidari[b,c], Mingjing Wang[a], Xu Chen[d], Xuehua Zhao[e,*]

[a] Department of Computer Science, Wenzhou University, Wenzhou 325035, China
[b] School of Surveying and Geospatial Engineering, College of Engineering, University of Tehran, Tehran, Iran
[c] Department of Computer Science, School of Computing, National University of Singapore, Singapore
[d] School of Electrical and Information Engineering, Jiangsu University, Zhenjiang 212013, China
[e] School of Digital Media, Shenzhen Institute of Information Technology, Shenzhen 518172, China

ARTICLE INFO

Keywords:
Solar module
Parameter estimation
Sine cosine algorithm
Simplex method
Opposition-based learning mechanism

ABSTRACT

Identifying the optimum parameters of photovoltaic models based on the measured current-voltage info is a vital step in monitoring, simulating, and optimizing the photovoltaic systems. We need efficient optimizers to reliably obtain the best model's parameters. In this study, a novel optimizer is proposed to effectively approximate the unknown parameters of solar cells and PV modules. The proposed ISCA is constructed based on the exploratory and exploitative cores of the sine cosine algorithm (SCA). Also, it is enhanced using the Nelder-Mead simplex (NMs) concept and the opposition-based learning (OBL) scheme. In ISCA, NMs method can guarantee the population's intensification and enhance the exploitation ability. In addition, the opposition-based learning scheme can improve the diversification of the population, which ensures a more steady balance between exploitation and exploration trends. The theory and structure of this algorithm are concise; therefore, it can be implemented easily. The developed ISCA is utilized to realize the unidentified parameters of the single diode, double diode, and photovoltaic module. Inclusive results and statistical analyses imply that the ISCA is superior to most of the reported techniques with regard to the accuracy of concluding solutions and convergence ratio. The results indicate that the proposed method can be treated as an effective, promising tool for parameter detection of the solar cells modules in dealing with practical cases.

1. Introduction

To reduce the use of fossil-based energies and their harms such as air pollution, we need to use new environmental sources of energy [1]. There are several renewable energy sources such as wave, nuclear, tidal, wind and so on; one of those sources with the most potential is the solar energy due to its property of wide readiness and cleanliness. Solar photovoltaic systems (PV) have been widely used in recent years and the sharp growth is still continuing [2,3], which can directly change the solar energy into electricity and supply power. However, reality is that PV systems are usually exposed to severe outdoor environmental cases and their PV arrays are not always efficient, which will have negative impacts on the productivity of solar systems [4]. Consequently, it is crucial to estimate the real performance of PV arrays in operation to simulate, manage, and optimize these systems. For this aim, we often use a truthful model in terms of measured current-voltage files [5]. The PV models can be constructed by two steps of mathematical model design and identification of parameters [6,7]. Various models have been proposed to deal with PV systems [8]. The single diode model (SDM) and the double diode model (DDM) are the most employed models for realizing real-world cases [9]. In addition, the actual behavior of PV models is basically decided by their unknown parameters. These parameters are extremely unstable and unpredictable when these models are faced with aging, breakdown, and volatile operating situations. Estimating these unknown parameters is a necessary stage in simulating, controlling, and optimizing these systems. Hence, we are witnessing the emergence of various computing techniques designed to deal with this problem [10,11].

We can develop an optimization model for this problem using a proper objective function. Many problems in engineering can be solved using an efficient algorithm and a mathematical model [12–16]. The measured current-voltage records are inevitably noisy. Hence, the objective function will form a multimodal topography [17,18]. Researchers have concentrated on this task based on different techniques.

* Corresponding author.
E-mail addresses: chenhuiling.jlu@gmail.com (H. Chen), js_1307@163.com (S. Jiao), as_heidari@ut.ac.ir, aliasgha@comp.nus.edu.sg, t0917038@u.nus.edu (A.A. Heidari), wangmingjing.style@gmail.com (M. Wang), xuchen@ujs.edu.cn (X. Chen), lcrlc@sina.com (X. Zhao).

https://doi.org/10.1016/j.enconman.2019.05.057
Received 27 December 2018; Received in revised form 16 May 2019; Accepted 18 May 2019
Available online 29 May 2019
0196-8904/

Some of them have used deterministic methods to deal with these tasks such as works at [19] and Newton method [20]. The deterministic methods are often based on gradient technique and perform well in local search. Unfortunately, these methods are easy to be trapped in a local optimum. Furthermore, deterministic techniques have numerous restrictions such as convexity and differentiability of the target function. They are extremely sensitive to initial situations. Note that the efficiency may be weaker when the initial solution is unsatisfactory. As an alternative, metaheuristic techniques have attracted many researchers [21–28]. In the past years, a great deal of research works has employed these methods or their variants to identify the PV models' parameters. Ishaque et al. [29] presented a penalty based differential evolution (PDE) to realize this problem at various environmental situations, while Jiang et al. [30] proposed an improved dynamic differential evolution (IADE). Huang et al. [31] designed a chaos particle swarm algorithm (CPSO) for this task. El-Naggar et al. [32] used original simulated annealing (SA) for estimation parameters. Dkhichi et al. [33] developed levenberg–marquardt algorithm combined with simulated annealing (LMSA) for solar cell parameters estimation. Rajasekar et al. [34] adopted the bacterial foraging algorithm (BFA) to simulate the characteristic of the solar PV. Oliva et al. [35] used artificial bee colony optimization (ABC) for solar cell estimation. Askarzadeh et al. [36] designed artificial bee swarm optimization algorithm (ABSO) for parameters identification of solar cell models and harmony search-based algorithms (IGHS) also was proposed this team [37]. Allam et al. [38] presented using month flame optimizer (MFO) to identify of parameters in three diode model. Five variants of BFA were constructed by Awadallah [39] in order to understand the parameters of the PV module based on nameplate info. Xu et al. [40] proposed a hybrid flower pollination algorithm (GOFPANM) for this task. Nunes et al. [41] presented a collaborative swarm intelligence to estimate PV parameters. Abbassi et al. [42] designed an efficient salp swarm-inspired algorithm (SSA) for parameters identification of photovoltaic cell models. A chaotic heterogeneous comprehensive learning particle swarm optimizer was developed by Yousri et al. [43] and it was applied to PV parameters estimation. Although these algorithms or their variants have shown superior and reliability compared to other deterministic techniques, further improvements are still required [38,44–46]. For example, based on no free lunch (NFL) theorem [47], there is no "universally best optimizer" for solving all possible problems. Moreover, most of the metaheuristic methods need user-defined parameters [46,48,49]. This fact is not an advantage because if we set them inaccurately, it will lead to stagnation drawback and immature convergence. In addition, based on the topography of decision space, the algorithm may easily fall into deceptive optima. In this case, they will not be able to enhance the quality of solutions by more iteration. On the other side, the common design of each algorithm makes it available to optimize some specific problems. For instance, in the case of the conventional DE or its variants, their special crossover operator increases the chance of finding more high-quality solutions, especially in dealing with multimodal problem landscapes [29]. Finally, the objective function of the PV parameters estimation task is nonlinear and multimodal, which contains multiple local optima. This fact is another challenge that makes this problem harder to be solved. Hence, developing a promising technique that is able to efficiently solve this multimodal problem and return accurate parameters of PV models is still a complex and challenging task.

The SCA is a novel optimizer for realizing continuous problems [50]. This algorithm creates multiple initial agents to oscillate with regard to the best agent based on some simple rules in trigonometry. The exploration and exploitation of the search space in different milestones of optimization are synchronously emphasized by several random and adaptive variables [51]. Due to its simplicity, SCA has attracted attention for solving practical tasks such as feature selection [52], neural networks [53,54], short-term hydrothermal scheduling [55], multi-objective problems [56], local sequence alignment [57] and object tracking [51]. However, SCA still has some deficiencies [58]. The first is that the different regions of the search may not be explored, thoroughly. In SCA, only the intuitionistic information of population is employed to direct the agents to the next population, which is not sufficient. This functionality cannot guarantee the diversity of swarm. Therefore, the exploratory trends of conventional SCA are not satisfactory in some problems. The second is that the intensification of the population can still be enhanced using more efficient local search operators. We see that the favorable zones of the feature space need to be exploited once sine and cosine yield values between -1 and 1. Furthermore, up to now, we have not seen any research work related to SCA for dealing with the parameters identification tasks of PV modules. Therefore, this study will develop a multi-strategy enhanced sine cosine algorithm (ISCA) based on the Nelder-Mead simplex strategy (NMs) and the opposition-based learning (OBL) scheme. This new methodology can be utilized to realize the investigated models with satisfactory exploratory and exploitative capabilities. In order to verify the efficacy of the ISCA, several state-of-the-art algorithms such as BLPSO [59], CLPSO [60], ALCPSO [61], IJAYA [62] and GOTLBO [63] are employed to compare with the proposal on unknown parameters estimation problems of different PV models including the SDM, DDM, and photovoltaic modules. In addition, some recently published methods have also been considered as comparison methods. In addition, two practical datasets that are directly abstracted from manufacturer's data sheets are also used to test the proposed ISCA with different levels of temperature and irradiation. The competitive and statistical experimental results have demonstrated that the proposed ISCA can provide high-quality solutions and reveal an enhanced efficacy in terms of exploration and exploitation trends with superior and competitive results.

In short, the main contributions of this study are as follows:

(1) By integrating the characteristics of OBL mechanism and NMs strategy, a new enhanced sine cosine algorithm (ISCA) is proposed to tackle solar photovoltaic parameter identification problems.
(2) In the proposed ISCA, the exploitative trends are boosted based on the operators of NMs strategy and in the same time, the exploratory behaviors are enhanced based on OBL-based procedure, which leads to a more stable tradeoff between the exploration and exploitation capacities.
(3) The effectiveness of ISCA is substantiated based on comprehensive experiments and comparisons with many original and modified methods using different PV models.

This paper is structured as follows. The formulation of the problem is given in Section 2. Section 3 presents the proposed method at length. The experiments are given in Section 4. Discussion on the results is presented in Section 5. Section 6 displays the conclusion and future works.

2. Problem definition

There are several models in the literature, which express the current-voltage characteristics of the solar cells and PV modules. Compared to other models, the SDM and DDM are the most frequently utilized models in practical applications. These models are described as follows.

2.1. Solar cell model

2.1.1. Single diode model

Due to the simplicity and accuracy, the SDM has been generally employed to elaborate on the characteristic of the solar cell. Fig. 1 vividly reveals the structure of this model. It can be seen from the figure that SDM contains a current source accompanied by a diode, a shunt resistor to show the leakage current, and a series resistor to consider the losses associated with the load current. The output current of this model

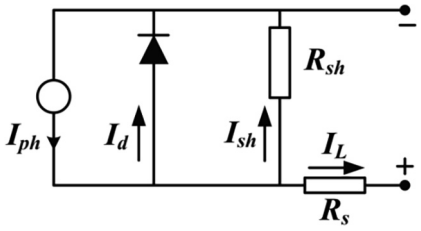

Fig. 1. Equivalent circuit diagram of SDM.

can be obtained as follow:

$$I_L = I_{ph} - I_d - I_{sh} \tag{1}$$

where I_L means the output current, I_{ph} is the photo-generated current, I_d denotes the diode current computed by Eq. (2), and I_{sh} means the shunt resistor current obtained by Eq. (3).

$$I_d = I_{sd} \bullet [\exp\left(\frac{q \bullet (V_L + R_S \bullet I_L)}{n \bullet k \bullet T}\right) - 1] \tag{2}$$

$$I_{sh} = \frac{V_L + R_S \bullet I_L}{R_{sh}} \tag{3}$$

where R_S and R_{sh} means the series and shunt resistances, respectively. V_L is the output voltage, I_{sd} means the reverse saturation current of the diode, n denotes the diode ideality factor, k is the Boltzmann constant ($1.3806503 \times 10^{-23}$J/K), q denotes the magnitude of the charge on an electron ($1.60217646 \times 10^{-19}$C), and the parameter T indicates the cell temperature in Kelvin. Consequently, Eq. (1) can be readjusted as follow:

$$I_L = I_{ph} - I_{sd} \bullet \left[\exp\left(\frac{q \bullet (V_L + R_S \bullet I_L)}{n \bullet k \bullet T}\right) - 1\right] - \frac{V_L + R_S \bullet I_L}{R_{sh}} \tag{4}$$

According to Eq. (4), five unknown parameters (I_{ph}, I_{sd}, R_S, R_{sh}, n) existed in the SDM. Accurate approximation of these parameters is crucial to show the performance of this solar cell, which can be obtained by an optimizer.

2.1.2. Double diode model

As we all know, the SDM pays no attention to the impact of the recombination current loss in the depletion region. Therefore, a more precise model namely DDM is proposed as shown in [64] when taking this loss into consideration. There are two diodes along with the current basis and a shunt resistance to shunt the photo-generated current basis. One of them is treated as a rectifier and another one is utilized to simulate the charge recombination current and some non-idealities. The equivalent circuit is shown in Fig. 2 and the output current is fulfilled in Eq. (5).

$$I_L = I_{ph} - I_{d1} - I_{d2} - I_{sh} = I_{ph} - I_{sd1} \bullet \left[\exp\left(\frac{q \bullet (V_L + R_S \bullet I_L)}{n_1 \bullet k \bullet T}\right) - 1\right] - I_{sd2} \bullet \left[\exp\left(\frac{q \bullet (V_L + R_S \bullet I_L)}{n_2 \bullet k \bullet T}\right) - 1\right] - \frac{V_L + R_S \bullet I_L}{R_{sh}} \tag{5}$$

where I_{sd1} and I_{sd2} are the diffusion and saturation currents, respectively, n_1 and n_2 both mean the diffusion and recombination diode ideality factors. It can be seen from Eq. (5) that seven unknown parameters (I_{ph}, I_{sd1}, I_{sd2}, R_S, R_{sh}, n_1, n_2) in this DDM, which are all needed to be identified to acquire the essential performance of the solar cell.

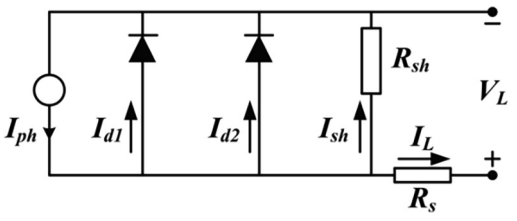

Fig. 2. Equivalent circuit diagram of DDM.

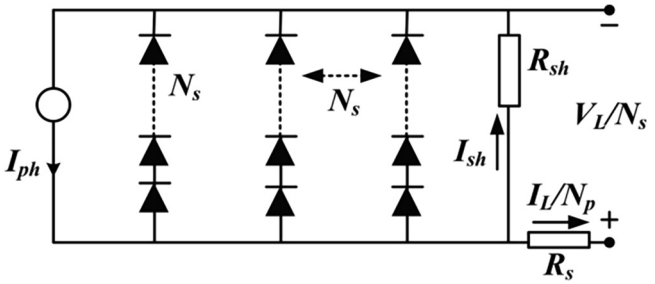

Fig. 3. Equivalent circuit diagram of the PV module.

2.2. PV module model

In the practical cases, the PV module model typically involves some solar cells as series and/or in parallel. Fig. 3 exhibits the corresponding circuit of the single diode PV module, and the output current is given as Eq. (6).

$$I_L/N_p = I_{ph} - I_{sd} \bullet \left[\exp\left(\frac{q \bullet (V_L/N_S + R_S \bullet I_L/N_P)}{n \bullet k \bullet T}\right) - 1\right] - \frac{V_L/N_S + R_S \bullet I_L/N_P}{R_{sh}} \tag{6}$$

where N_p and N_S mean the number of solar cells in parallel and series, respectively. The same situation can be observed as abovementioned SDM, the unknown parameters (I_{sh}, I_{sd}, R_S, R_{sh}, n) are also needed to be identified to promote the performance of the model.

2.3. Objective function

To realize the optimum models, the fundamental aim is to find the optimal parameters in each model. The purpose is to minimize the variance between the photo-generated and planned current data. The function of error for every pair of photo-generated and gotten the current data point in this study is computed for SDM and DDM as Eqs. (7) and (8), respectively.

$$f_k(V_L, I_L, x) = I_{ph} - I_{sd} \bullet \left[\exp\left(\frac{q \bullet (V_L + R_S \bullet I_L)}{n \bullet k \bullet T}\right) - 1\right] - \frac{V_L + R_S \bullet I_L}{R_{sh}} - I_L$$
$$x = \{I_{ph}, I_{sd}, R_S, R_{Sh}, n\} \tag{7}$$

$$f_k(V_L, I_L, x) = I_{ph} - I_{sd1} \bullet \left[\exp\left(\frac{q \bullet (V_L + R_S \bullet I_L)}{n_1 \bullet k \bullet T}\right) - 1\right] - I_{sd2} \bullet \left[\exp\left(\frac{q \bullet (V_L + R_S \bullet I_L)}{n_2 \bullet k \bullet T}\right) - 1\right] - \frac{V_L + R_S \bullet I_L}{R_{sh}} - I_L \quad x$$
$$= \{I_{ph}, I_{sd1}, I_{sd2}, R_S, R_{Sh}, n_1, n_2\} \tag{8}$$

For a comprehensive evaluation of the PV module, the root mean square error (RMSE) is utilized to quantify the overall difference as shown in Eq. (9), N means the number of experimental data, this metric is commonly treated as the objection function [65]. Therefore, in this study, the optimization procedure is concentrated on minimizing the objection function RMSE (x) according to tuning the solution vector$x$ in the whole iterations.

$$RMSE(x) = \sqrt{\frac{1}{N}\sum_{k=1}^{N} f_k(V_L, I_L, x)^2} \quad k = 1, 2, \cdots, N. \tag{9}$$

3. The proposed algorithm

3.1. Basic sine cosine algorithm

SCA is a stochastic optimizer based on the simple mathematical functions sine and cosine. For a more detailed description of this algorithm, refer to the original article [50]. The main step of an optimizer is known to be the formulation of the position updating equation. In SCA, the position updating equation is constructed based on sine and cosine as follows;

$$X_i^{t+1} = \begin{cases} X_i^t + r_1 \times \sin(r_2) \times |r_3 P_i^t - X_i^t|, & r_4 < 0.5 \quad (10.1) \\ X_i^t + r_1 \times \cos(r_2) \times |r_3 P_i^t - X_i^t|, & r_4 \geq 0.5 \quad (10.2) \end{cases}$$

where X_i^t means the position of the current candidate agent in i_th dimension at t_th iteration, $r_1/r_2/r_3$ are random numbers, P_i means the position of the destination point in i_th dimension, $||$ is the absolute value, r_4 is a random number in [0, 1]. The parameter $r_1$controls the new position's region, which may be either in the space between the agent and destination or outside it. The parameter r_2 decides the distance towards or outwards the endpoint. The parameter r_3 generates a random weight for the destination to highlight ($r_3 > 1$) or decrease ($r_3 < 1$) the impact of the endpoint in defining the distance. The parameter r_4 is a random value in [0, 1] and equally switches between the sin and cosine-based updating rules. To help SCA for finding a well-balanced state between the exploratory and exploitative tendencies, the parameter r_1 is chosen adaptively as follows:

$$r_1 = a - t\frac{a}{T} \quad (11)$$

where t means the current iteration, T is the maximum number of iterations and a is a constant and set to 2. The pseudo code of this algorithm is presented as follows:

Algorithm 1: The pseudo code of SCA

Initialize a set of search solutions (X);
Do
  Evaluate each of the search solutions by the objective function;
  Update the best solution obtained so far ($P = X^*$);
  Update the parameters of r_1, r_2, r_3 and r_4;
  Update the position of each search solution agent using Eq. (10);
While ($t < T$)
Return the best solution.

3.2. Nelder-Mead simplex method (NMs)

To deal with unconstrained minimization scenarios, the NMs method was originally emerged [66]. This special technique can solve the objective function without its derivatives and many scientific and practical engineering problems [67,68] have been overcome according to this method. The NMs method can be treated as an iterative algorithm. For example, NMs would start from a simplex formed by $D + 1$ initial vertices when faced with D dimensional minimization function. Some vertices which are worse than newly generated vertices can be taken place in each iteration, thus a new simplex is fulfilled. With the constant iteration, the simplex would be directed and closer to the best solution.

The details of the NMs method can be abstracted as six steps in each iteration in following [66]:

Step1: With the order of fitness values are ascending, we need to sort and number all the vertices based on Eq. (12):

$$f(x_1) \leq f(x_2) \leq f(x_3) \leq \cdots \leq f(x_D) \leq f(x_{D+1}) \quad (12)$$

Step2: By using Eq. (13), calculate the reflection point x_r and obtain the fitness function value$f(x_r)$. Replace x_{D+1} with x_r and execute step 6, if $f(x_1) \leq f(x_r) \leq f(x_D)$; if $f(x_1) > f(x_r)$, then, perform step 3; if $f(x_D) \leq f(x_r)$, then, execute the step 4;

$$x_r = (1 + \alpha)\bullet\bar{x} - \alpha\bullet x_{D+1} \quad (13)$$

where α shows a factor utilized for the reflection, $\bar{x}$ is the centering point of vertices except x_{D+1}, which is attained by Eq. (14):

$$\bar{x} = \sum_{i=1}^{n} x_i/D \quad (14)$$

Step 3: Determine the expansion pointx_e based on Eq. (15) and the fitness function value is $f(x_e)$. If$f(x_e) \leq f(x_r)$, then x_{D+1} is replaced by x_e; else $x_{D+1}$is replaced by x_r. Then, perform step 6.

$$x_e = (1 - \beta)\bullet\bar{x} + \beta\bullet x_r \quad (15)$$

where β shows a factor of expansion.

Step 4: if$f(x_r) < f(x_{D+1})$, the external contraction point $x_{oc}$is calculated by using Eq. (16) and the corresponding fitness value is $f(x_{oc})$; else the inside contraction point x_{ic} is calculated by Eq. (17) and the corresponding fitness value is $f(x_{ic})$;

$$x_{oc} = (1 - \gamma)\bullet\bar{x} + \gamma\bullet x_r \quad (16)$$

$$x_{ic} = (1 - \gamma)\bullet\bar{x} + \gamma\bullet x_{D+1} \quad (17)$$

where γ is the contraction factor in Eqs. (16) and (17).

Once, the x_{oc} is generated, if $f(x_{oc}) < f(x_r)$, then $x_{D+1}$is replaced by x_{oc}, and perform step 6; else, run the step 5. For the case that x_{ic} is generated, if $f(x_{ic}) < f(x_{D+1})$, then, replace x_{D+1} with x_{ic}, and accomplish step 6; otherwise, execute step 5;

Step 5: altogether vertices except x_1 are shrunk based on Eq. (18) to generate a new simplex and jump to step 6.

$$V_i = \delta\cdot x_i + (1 - \delta)\cdot x_1, \; i = 2, \ldots, D + 1 \quad (18)$$

where δ means a shrinkage factor.

Step 6: if the cut-off condition is met, stop the searching process; else, enter the subsequent iteration.

3.3. OBL mechanism

The OBL mechanism was originally designed in 2005 [69]. This special technique has been further presented [70–72] since it was proposed, which has also been proved to be an operative tactic for humanizing the searching trends of meta-heuristic optimizers. This technique is derived from the concurrently estimating the matching opposite pairs of the base agents to increase the chance of meeting an agent with a better fitness value. The opposite of a real number $x \in [l_b, l_u]$ can be given by $\vec{x}$ as follows:

$$\bar{x} = l_b + l_u - x \quad (19)$$

where $l_b$and l_u are the lowest and upper bounds. In the multi-dimensional space, the description of x can be generated as shown in a previous study [69]. It was assumed that $x_i = \{x_{i1}, x_{i2}, x_{i3}, \cdots, x_{ij}\}$ and $x_{ij} \in [l_{bj}, l_{uj}]$, where $j = 1, 2, \cdots, n$, and the opposite point was as follows:

$$\bar{x_i} = \{\bar{x_{i1}}, \bar{x_{i2}}, \ldots, \bar{x_{ij}}\}, \quad \bar{x_{ij}} = l_{bj} + l_{uj} - x_{ij} \quad (20)$$

In the process of optimization, the opposite point $\bar{x_i}$ was replaced by the corresponding solution x_i based on the fitness function. If $f(x_i)$ was better than $f(\bar{x_i})$, than the x_i was not changed; otherwise, $x_i = \bar{x_i}$. In other words, the position of the population was updated based on the better values of x_j and $\bar{x_i}$.

3.4. The proposed algorithm

The developed methodology in this work enhances the SCA, with the NMs method and the OBL scheme. The SCA can maintain a relatively ideal property in terms of the balance between exploration and exploitation, the NMs method can further search the neighborhood as an effective local search technique [67], the OBL mechanism can deeply

explore the whole decision space and sidestep the local optima, simultaneously.

Initially, the OBL mechanism is used inside the original SCA to expand the extents of the search space and boost the exploratory trends. At length, the algorithm firstly executes the base strategies of the SCA for evolving the swarm, and then transfer to execute the OBL mechanism. The OBL part can be given along these lines. Assume that the present set of solutions in the SCA is $X(t)$, which comprises N candidate agents as exhibited Eq. (21). t is the current iteration and D means the dimensions of the pending task. The opposite position of $X(t)$ is given as Eq. (22) and calculated according to Eq. (19). And then fulfill the best N solutions from $X(t)$ and $\bar{X}(t)$ which would be utilized to replace the current population.

$$X(t) = \begin{bmatrix} x_1 \\ x_2 \\ \vdots \\ x_N \end{bmatrix} = \begin{bmatrix} x_{1,1} & \cdots & x_{1,D} \\ \vdots & \ddots & \vdots \\ x_{N,1} & \cdots & x_{N,D} \end{bmatrix} \tag{21}$$

$$\bar{X}(t) = \begin{bmatrix} \bar{x_1} \\ \bar{x_2} \\ \vdots \\ \bar{x_N} \end{bmatrix} = \begin{bmatrix} \bar{x_{1,1}} & \cdots & \bar{x_{1,D}} \\ \vdots & \ddots & \vdots \\ \bar{x_{N,1}} & \cdots & \bar{x_{N,D}} \end{bmatrix} \tag{22}$$

Then, the NMs mechanism is incorporated and located after the OBL method in order to perform exploitive steps in the potential neighborhood zones found by the original SCA. In detail, the best agent in the current swarm after OBL operating would be selected and used to construct a primary simplex. Then, the simplex is updated according to the NMs simplex mechanism for μ iterations. The μ is a vital parameter which would cause that the NMs method would be overemphasized when its value is too large, contrarily this mechanism could not exert its local search ability thoroughly. Through repeated experiments, its value is chosen as$D + 1$. And then, the NMs simplex method will be carried out for μ iterations and switched back to the original SCA. Furthermore, such an elite selection is adapted to select a better solution from the current best solution and its vertices of the updated simplex to form the new best solution. The flowchart of the proposed method can be seen in Fig. 4.

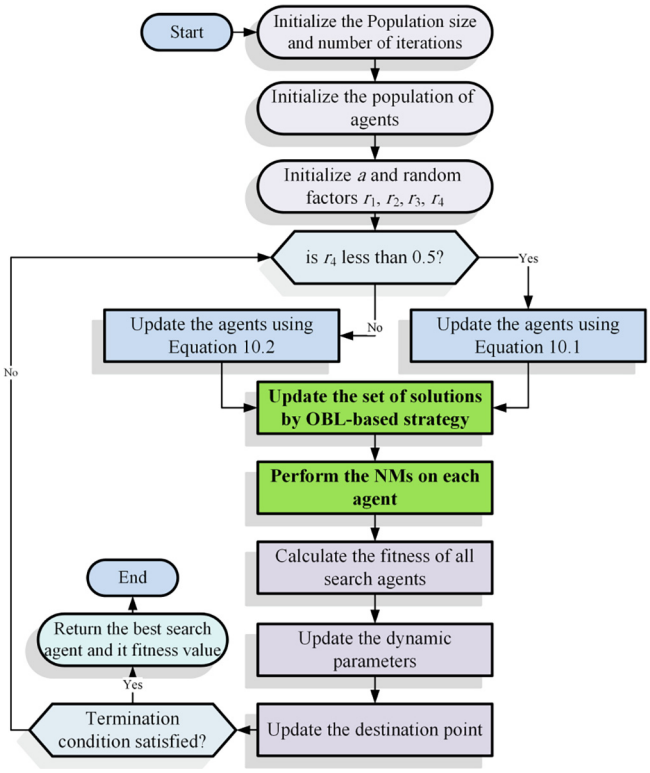

Fig. 4. Flowchart of the proposed algorithm.

4. Simulation results and analysis

In order to substantiate the performance of the proposal, three parameters identification problems abstracted from [20] are firstly executed by the ISCA in this study. These problems are composed of two models for SDM and DDM and a case study for a PV module, in which a 57 mm diameter commercial R.T.C. France silicon solar cell working at an irradiance of 1000 W/m^2 and a temperature of 33 °C, and a solar unit named Photowatt-PWP201 covers 36 polycrystalline silicon cells in sequence functioning at an irradiance of 1000 W/m^2 and a temperature of 45 °C. This dataset has been widely employed to verify the capability of new methods [36,40,64]. For a straight and fair judgment, the same lower and upper limitations of all pending parameters are adopted as the previous literature and the detailed descriptions are given in Table 1. Furthermore, in order to thoroughly verify the capability of the ISCA, several other state-of-the-art algorithms including BLPSO [59], CLPSO [60], ALCPSO [61], IJAYA [62] and GOTLBO [63] are employed to compare them on unknown parameters estimation problems of different PV models including the SDM, DDM, and photovoltaic modules. These algorithms are population-based metaheuristic algorithms that showed high potential for continuous problems. Wilcoxon rank sign test with a significant level of 0.05 is utilized to compare the significance between ISCA and these competitors. Symbols '+', '−' and '=' indicates that ISCA is significantly better than, worse than, or similar to its competitor, respectively. Moreover, some recently published methods about corresponding models are considered in this study. These methods all have received considerable attention in current problems and the corresponding parameters are the same as their corresponding citations. In addition, two datasets from the manufacturer's data sheet are also utilized to affirm the efficacy of the ISCA, and different levels of irradiation and different temperature are also considered.

Table 1
Bounds of parameters for different PV models.

Parameters	Single diode/double diode		PV module	
	Lower bound	Upper bound	Lower bound	Upper bound
I_{ph}(A)	0	1	0	2
I_{sd}, I_{sd1}, I_{sd2}(μA)	0	1	0	50
R_s(Ω)	0	0.5	0	2
R_{sh}(Ω)	0	100	0	2000
n, n_1, n_2	1	2	1	50

In this study, ISCA is implemented in MATLAB R2014a and is tested with 30 independent rounds in a server with Windows 10 system, Intel Xeon 2.60 GHz CPU, and 128 GB RAM. The maximum number of evaluations (NFEs) is set 10,000 for SDM solar cell case, DDM case and PV module case. According to the above description, Eq. (8) is employed to check the excellence of each solution generated by an execution algorithm.

4.1. Results on the SDM case

Fig. 5 shows the I–V characteristics and P–V characteristics of the experimental data and simulated data achieved by ISCA for SDM. We see that the estimated curves of the resulted model are highly in coincidence with those for the experimental dataset used in this study over the whole voltage range. Fig. 6 vividly exhibits an index for the error values of the simulated and experimental current data of SDM with IAE values and RE values, respectively. All values of IAE are smaller than 2.508E−03 and all RE's values are inside [−2.00E−02, 1.47E−01],

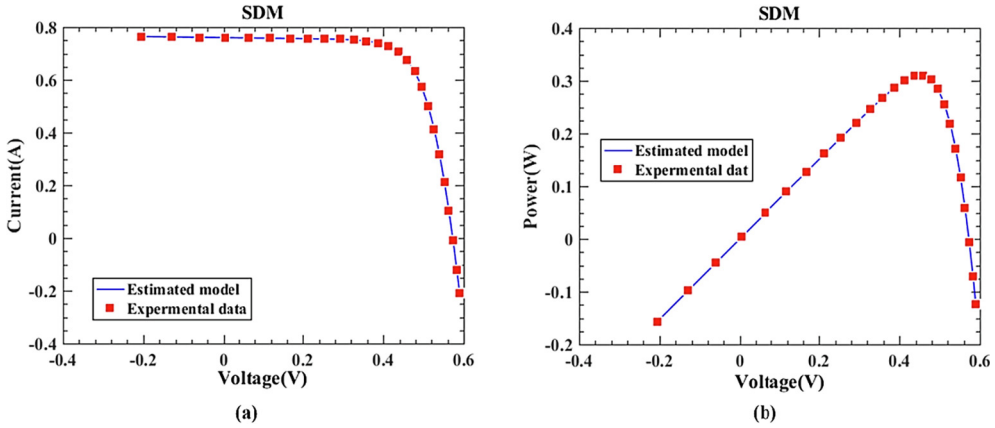

Fig. 5. Comparisons between the experimental and simulated data returned by ISCA for SDM (a) I–V characteristics; (b) P–V characteristics.

which demonstrates that the real performance of the SDM can be accurately simulated by the proposed ISCA. Table 2 further records the detailed statistical results of the individual absolute errors based on the current and power for the experimental and simulated data on SDM and the sum of the values of IAE are 2.15E−02 and 8.73E−03, respectively. Then, we see that the accuracy of the estimated parameter in SDM can be guaranteed.

Table 3 vividly records the statistical results including the minimum, median, mean, maximum, as well as the standard deviation (SD) of RMSE values. These results are obtained using the proposed ISCA and other competitors including the BLPSO, CLPSO, ALCPSO, IJAYA, and GOTLBO for SDM based on 30 runs. From Table 3, it can be observed that based on the minimum, median, mean, and maximum of RMSE values, the proposed ISCA obtains the best results. This finding means that the OBL-based ISCA achieves the best solution for this task. In terms of the standard deviation of RMSE, ISCA has an obvious superiority over all other algorithms. This indicates that the ISCA is the most reliable and stable method among these competitors. In addition, according to the Wilcoxon rank sum test, we see that the results of ISCA are significantly different compared to other algorithms. Fig. 7 plots the convergence graphs of all these competitors. Based on convergence trends, we observe that the proposed ISCA has shown a faster convergence speed compared to all other techniques for this case. We can see methods such as BLPSO and CLPSO show some stagnation behaviors, while the GOTLBO is the second top method in terms of convergence rate.

For this case, Table 4 shows the optimal model's parameters and RMSE values estimated by ISCA and several published methods including CPSO, PS, LMSA, ABC, ABSO, and GOFPANM. It can be observed from Table 4 that ISCA, together with GOFPANM obtains the best RMSE value 9.8602E−04 among all these competitors on this SDM. We see that ABC achieves the second best RMSE value 9.8620E−04, followed by LMSA, GOTLBO, ABSO, PS, and CPSO. Based on the above descriptions, a preliminary conclusion can be drawn that the proposal ISCA may be treated as a potential tool for identifying appropriate parameters of SDM case.

4.2. Results on the DDM case

In this part, we investigate the results of the DDM case. Fig. 8 illustrates the I–V and P–V characteristics of the experimental and simulated data found by ISCA for DDM. As it is shown, similarly to what we observed for the SDM problem, the I–V and the P–V curves of the resulted model are obviously in accordance with the experimental dataset used in this study over the whole voltage range.

Fig. 9 shows the error index values of the simulated and experimental current data of DDM with IAE values and RE values, respectively. All the IAE are smaller than 2.54E−03 and all RE values are located inside [−2.03E−02, 1.37E−01], which shows that the real performance of the DDM can be accurately estimated by the proposed ISCA. Table 5 describes the detailed experimental results of the IAE on DDM and the sum of the values of IAE are 1.66E−05 and1.86E−06, respectively.

Table 6 compares the statistical results for the DDM case. From Table 6, it can be seen that ISCA achieve the best results in terms of minimum, mean, maximum and standard deviation of RMSE. According to the Wilcoxon rank sum test, ISCA is significantly better than all these competitors in this case. Fig. 10 plots the convergence graphs of all these competitors on DDM case. It can be seen that GOTLBO is able to reveal a faster convergence rate than ISCA at the primary part of the

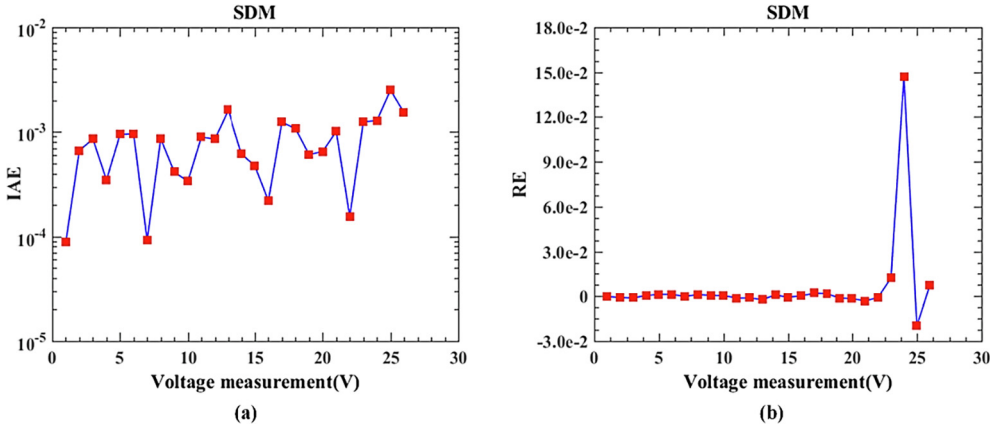

Fig. 6. Error index values of the simulated and the experimental current data for SDM (a) IAE's values; (b) RE's values.

Table 2
IAE of ISCA on SDM.

Item	Measured data		Simulated current data		Simulated power data	
	$V(V)$	$I(A)$	$I_{sim}(A)$	$IAE_I(A)$	$P_{sim}(W)$	$IAE_P(W)$
1	−0.2057	0.7640	0.764087776	8.77756E−05	−0.157172855	1.80554E−05
2	−0.1291	0.7620	0.762663137	0.000663137	−0.098459811	8.56109E−05
3	−0.0588	0.7605	0.761355338	0.000855338	−0.044767694	5.02939E−05
4	0.0057	0.7605	0.760154004	0.000345996	0.004332878	1.97218E−06
5	0.0646	0.7600	0.759055205	0.000944795	0.049034966	6.10337E−05
6	0.1185	0.7590	0.758042327	0.000957673	0.089828016	0.000113484
7	0.1678	0.7570	0.757091622	9.16216E−05	0.127039974	1.53741E−05
8	0.2132	0.7570	0.756141319	0.000858681	0.161209329	0.000183071
9	0.2545	0.7555	0.755086815	0.000413185	0.192169594	0.000105156
10	0.2924	0.7540	0.753663809	0.000336191	0.220371298	9.83024E−05
11	0.3269	0.7505	0.751390884	0.000890884	0.245629680	0.000291230
12	0.3585	0.7465	0.747353756	0.000853756	0.267926322	0.000306072
13	0.3873	0.7385	0.740117112	0.001617112	0.286647358	0.000626308
14	0.4137	0.7280	0.727382100	0.000617900	0.300917975	0.000255625
15	0.4373	0.7065	0.706972513	0.000472513	0.309159080	0.000206630
16	0.4590	0.6755	0.675280004	0.000219996	0.309953522	0.000100978
17	0.4784	0.6320	0.630758124	0.001241876	0.301754687	0.000594113
18	0.4960	0.5730	0.571928218	0.001071782	0.283676396	0.000531604
19	0.5119	0.4990	0.499606895	0.000606895	0.255748770	0.000310670
20	0.5265	0.4130	0.413648693	0.000648693	0.217786037	0.000341537
21	0.5398	0.3165	0.317510037	0.001010037	0.171391918	0.000545218
22	0.5521	0.2120	0.212154893	0.000154893	0.117130716	8.55164E−05
23	0.5633	0.1035	0.102251286	0.001248714	0.057598149	0.000703401
24	0.5736	−0.0100	−0.008717559	0.001282441	−0.005000392	0.000735608
25	0.5833	−0.1230	−0.125507430	0.002507430	−0.073208484	0.001462584
26	0.5900	−0.2100	−0.208472356	0.001527644	−0.122998690	0.000901310
Sun of IAE	NA	NA	NA	0.021526959	NA	0.008730758

iteration but ISCA performs a process of accelerating convergence trend. Finally, it goes beyond the GOTLBO because it performs a smoother transition from exploration to exploitation. Therefore, the proposed ISCA can show a fast convergence speed compared to all other algorithms for DDM case.

For this problem, Table 7 shows the comparison results with several published methods including PS, SA, IGHS, ABC, ABSO, and GOFPANM. It can be seen that ISCA obtains the best RMSE value 9.8237E−04 among all these competitors on this DDM. GOFPANM obtains the second best RMSE value 9.823E−04, followed by GOTLBO, ABSO, ABC, IGHS, SA, and PS. Therefore, the proposed ISCA has shown a high potential for identifying the parameters of the DDM case.

4.3. Results on the PV model case

In this part, we investigate the results of the PV model case.

Fig. 11 records the I–V and P–V characteristics of the experimental data and simulated data attained by ISCA in dealing with the PV model. As it is shown in Fig. 11, the I–V and the P–V curves of the resulted model are in fairly good consistency with the experimental dataset used in this study over the whole voltage range.

Fig. 12 vividly shows the error index values of the simulated and experimental current data of SDM with IAE values and RE values, respectively. All the IAE values are smaller than 4.8328E−03 and all RE

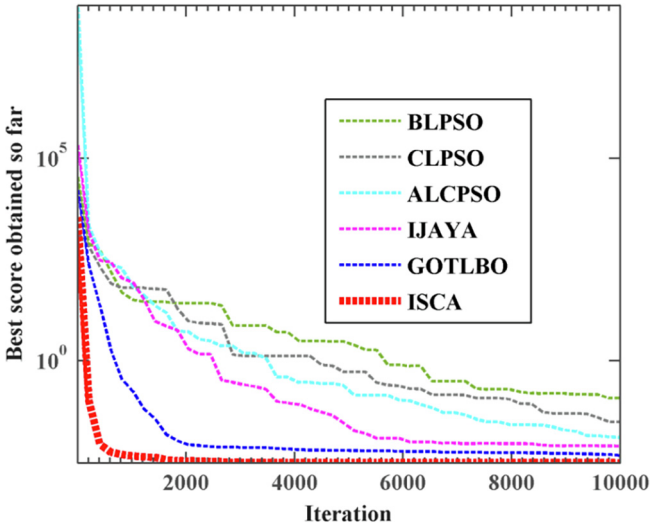

Fig. 7. Convergence graph of different algorithms for SDM.

Table 3
Statistical results of the RMSE values achieved by different algorithms for SDM.

Algorithm	RMSE					
	Min	Median	Mean	Max	SD	Sig
BLPSO	1.10417E−03	1.59394E−03	1.58543E−03	2.19554E−03	2.66193E−04	+
CLPSO	1.01347E−03	1.08407E−03	1.09114E−03	1.39910E−03	5.68626E−05	+
ALCPSO	1.01233E−03	1.21302E−03	2.1231E−03	3.22331E−03	6.18669E−05	+
IJAYA	1.44512E−03	1.39348E−03	1.20312E−03	1.82123E−03	2.45631E−04	+
GOTLBO	1.34432E−03	1.20322E−03	1.02903E−03	2.3454E−03	1.32134E−03	+
ISCA	7.34231E−04	6.32163E−04	7.23043E−04	7.45921E−04	1.30287E−06	

Table 4
Comparison among published different algorithms on SDM.

Item	CPSO	PS	LMSA	ABC	ABSO	GOFPANM	ISCA
I_{ph}(A)	0.7607	0.7617	0.76078	0.7608	0.7608	0.76077755	0.76077562
I_{sd}(μA)	0.4	0.998	0.31849	0.3251	0.30623	0.3230208	0.32301700
R_s(Ω)	0.0354	0.0313	0.03643	0.0364	0.03659	0.0363771	0.03637716
R_{sh}(Ω)	59.012	64.1026	53.32644	53.6433	52.2903	53.7185203	53.71821748
n	1.5033	1.6	1.47976	1.4817	1.47878	1.4811836	1.48118220
RMSE	1.3900E−03	1.4940E−02	9.8640E−04	9.8620E−04	9.9124E−04	9.8602E−04	9.8602E−04

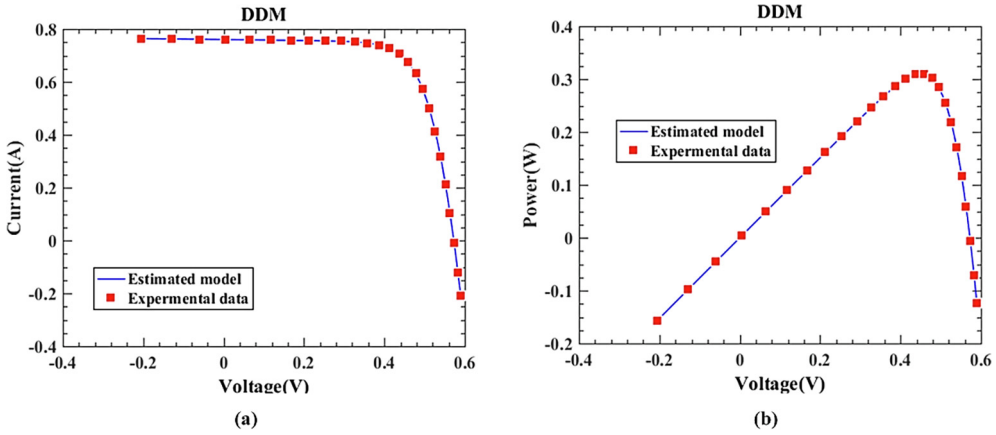

Fig. 8. Comparisons between the experimental and simulated data found by ISCA for DDM (a) I–V characteristics; (b) P–V characteristics.

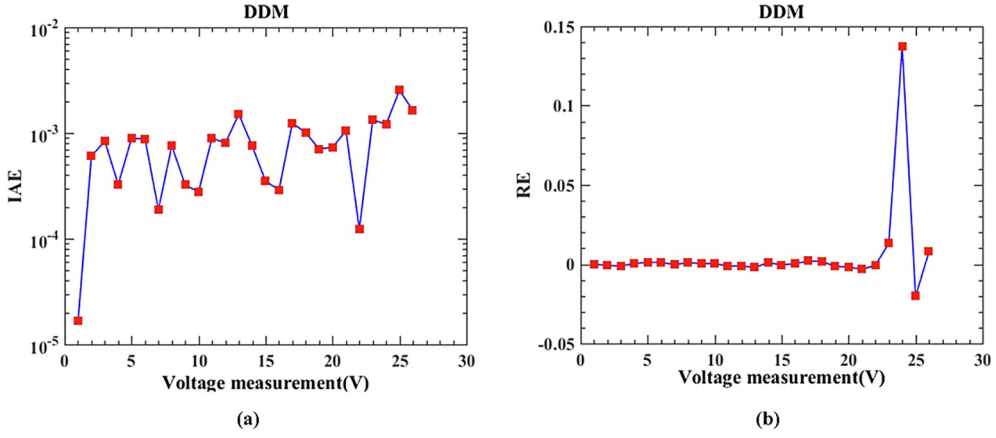

Fig. 9. Comparisons of the characteristics of the obtained model and the experimental data of DDM (a) I–V characteristics; (b) P–V characteristics.

values are located inside the range of [−3.91E−02, 5.0255E−02], which this observation verifies that the actual behavior of this PV model case can be accurately identified by the proposed ISCA. Table 8 further shows the detailed statistical results of the IAE on PV model and the values sum of IAE are 4.8924E−02 and 5.1689E−01, respectively. Here, the same sign can be seen in Table 10 and the accuracy of the estimated parameter in the PV model can be guaranteed.

Table 9 tabulates the statistical results achieved by the proposed ISCA and other competitors including the BLPSO, CLPSO, ALCPSO, IJAYA, and GOTLBO on PV module. According to the results recorded in Table 9, the performance of ISCA is very competitive for this PV modules. Based on the minimum RMSE, ISCA has the best solution among all these algorithms. Based on the Wilcoxon rank sum test, ISCA performs significantly better than all other competitors on this PV module. Fig. 13 vividly shows the convergence graph of different algorithms for the PV module. It can be observed from Fig. 13 that the proposed ISCA shows a superior rate in terms of convergence speed in comparison with other competitors on the PV module.

In order to further verify the efficacy of the ISCA, several published methods including Newton, PS, SA, the method in [73] and GOFPANM are employed to be compared. It can be found that the proposed ISCA finds the best RMSE value 2.4250E−03 among all these methods on this PV model case. We see that the GOFPANM achieves the second best RMSE value 2.4250E−03, followed by SA, CPSO, PS, the method in [73], and Newton. In a nutshell, the proposed ISCA has an obvious superiority over other competitors. Hence, it can be applied to identifying appropriate parameters of the PV diode model case.

In order to further identify the computational efficiency of ISCA, the average computational time of all competitors on three models is compared. Based on 30 independent runs, we recorded the average CPU time of each algorithm on each model and the results are shown in Fig. 14. It can be observed from Fig. 14 that each algorithm will spend different computational time in tackling each problem. We see that the ISCA is the fastest method with minimum time on each model, while the BLPSO requires the maximum time compared to other methods. We see that PSO-based algorithms generally consume more computational

Table 5
IAE of ISCA on DDM.

Item	Measured data		Simulated current data		Simulated power data	
	$V(V)$	$I(A)$	$I_{sim}(A)$	$IAE_I(A)$	$P_{sim}(W)$	$IAE_P(A)$
1	−0.2057	0.7640	0.763983413	1.65865E−05	−0.157151388	3.41185E−06
2	−0.1291	0.7620	0.762604097	0.000604097	−0.098452189	7.79890E−05
3	−0.0588	0.7605	0.761337700	0.000837700	−0.044766657	4.92567E−05
4	0.0057	0.7605	0.760173789	0.000326211	0.004332991	1.85940E−06
5	0.0646	0.7600	0.759107682	0.000892318	0.049038356	5.76438E−05
6	0.1185	0.7590	0.758121422	0.000878578	0.089837388	0.000104112
7	0.1678	0.7570	0.757188616	0.000188616	0.127056250	3.16497E−05
8	0.2132	0.7570	0.756243609	0.000756391	0.161231137	0.000161263
9	0.2545	0.7555	0.755177304	0.000322696	0.192192624	8.21261E−05
10	0.2924	0.7540	0.753722357	0.000277643	0.220388417	8.11829E−05
11	0.3269	0.7505	0.751399139	0.000899139	0.245632378	0.000293928
12	0.3585	0.7465	0.747301449	0.000801449	0.267907569	0.000287319
13	0.3873	0.7385	0.740010668	0.001510668	0.286606132	0.000585082
14	0.4137	0.7280	0.727246961	0.000753039	0.300862068	0.000311532
15	0.4373	0.7065	0.706850308	0.000350308	0.309105640	0.000153190
16	0.4590	0.6755	0.675210553	0.000289447	0.309921644	0.000132856
17	0.4784	0.6320	0.630760767	0.001239233	0.301755951	0.000592849
18	0.4960	0.5730	0.571994741	0.001005259	0.283709392	0.000498608
19	0.5119	0.4990	0.499706142	0.000706142	0.255799574	0.000361474
20	0.5265	0.4130	0.413733677	0.000733677	0.217830781	0.000386281
21	0.5398	0.3165	0.317546208	0.001046208	0.171411443	0.000564743
22	0.5521	0.2120	0.212122998	0.000122998	0.117113107	6.79069E−05
23	0.5633	0.1035	0.102163278	0.001336722	0.057548575	0.000752975
24	0.5736	−0.0100	−0.008791748	0.001208252	−0.005042946	0.000693054
25	0.5833	−0.1230	−0.125543429	0.002543429	−0.073229482	0.001483582
26	0.5900	−0.2100	−0.208371580	0.001628420	−0.122939232	0.000960768
Sun of IAE	NA	NA	NA	0.021300000	NA	0.008780000

Table 6
Statistical results of the RMSE values achieved by different algorithms for DDM.

Algorithm	RMSE					
	Min	Median	Mean	Max	SD	Sig
BLPSO	1.00692E−03	1.09482E−03	1.15977E−03	1.52063E−03	1.55923E−04	+
CLPSO	1.01243E−03	1.08407E−03	1.09114E−03	1.39910E−03	5.62326E−04	+
ALCPSO	1.34433E−03	2.52156E−03	2.5031E−03	3.768331E−03	2.66192E−04	+
IJAYA	1.37213E−03	1.45543E−03	1.78902E−03	1.98231E−03	1.32564E−04	+
GOTLBO	1.20232E−03	1.12312E−03	1.03530E−03	4.43212E−03	1.02312E−04	+
ISCA	9.8342E−04	9.83073E−04	9.83800E−04	9.86863E−04	1.65397E−06	

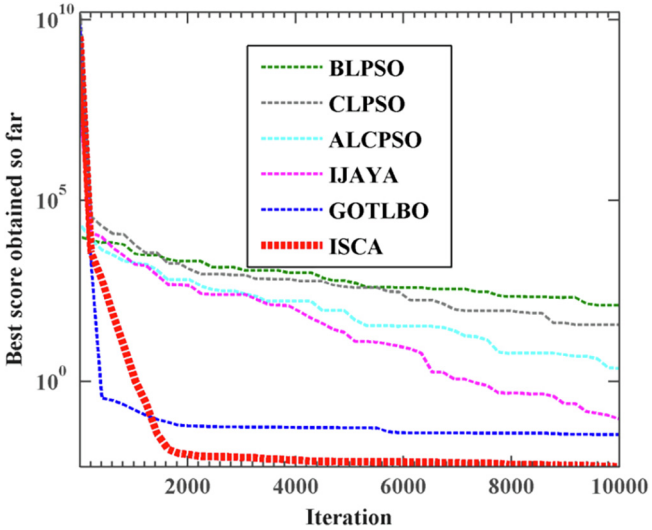

Fig. 10. Convergence graph of different algorithms for DDM.

time compared to other algorithms. There is a close competition between the ISCA and JAYA on DDM model but the ISCA is slightly faster. The compassion of time results verifies that the proposed ISCA can show a fairly fast performance when finding better results than other methods.

4.4. Results of ISCA for the data of the manufacturer's data sheet

In this part, we are interested to investigate the efficacy and reliability of the proposed ISCA in dealing with both SDM and DDM cases. These experiments are performed using the experimental info, which is abstracted from the manufacturer's data sheet of two PV modules. These datasets are composed of Thin-film (ST40) [74], Mono-crystalline (SM55) [75]. These two datasets have been often used to evaluate the property of the proposed method for parameter estimation of photovoltaic models. Fathy et al. [5] used only ST40 to investigate the property of imperialist competitive algorithm (ICA) for parameters estimation of photovoltaic models. Alam et al. [9] evaluated the capability of flower pollination algorithm (FPA) for this task based on both SM55 and ST40. Xu et al. also evaluated the property of modified FPA (GOFPANM) using these two datasets [40]. In addition, Yu et al. [76] proposed a performance-guided JAYA (PGJAYA) algorithm for parameter estimation of photovoltaic models. Their proposal was also strictly evaluated based on SM55 and ST40. These efforts show that the

Table 7
Comparison among published different algorithms based on DDM.

Item	PS	SA	IGHS	ABC	ABSO	GOFPANM	ISCA
I_{ph}(A)	0.7602	0.7623	0.7608	0.7608	0.76077	0.7607811	0.760781079
I_{sd1}(μA)	0.9889	0.4767	0.9731	0.0407	0.26713	0.7493467	0.74934632
I_{sd2}(μA)	0.0001	0.01	0.1679	0.2874	0.38191	0.2259743	0.22597411
R_s(Ω)	0.032	0.0345	0.0369	0.0364	0.03657	0.0367404	0.036740424
R_{sh}(Ω)	81.3008	43.1034	53.8368	53.7804	54.6219	55.485448	55.48542959
n_1	1.6	1.5172	1.9213	1.4495	1.46512	2.0000000	2.0000000
n_2	1.192	2	1.4281	1.4885	1.98152	1.4510168	1.45101691
RMSE	1.58E−02	1.664E−02	9.8635E−04	9.861E−04	9.834E−04	9.8248E−04	9.8237E−04

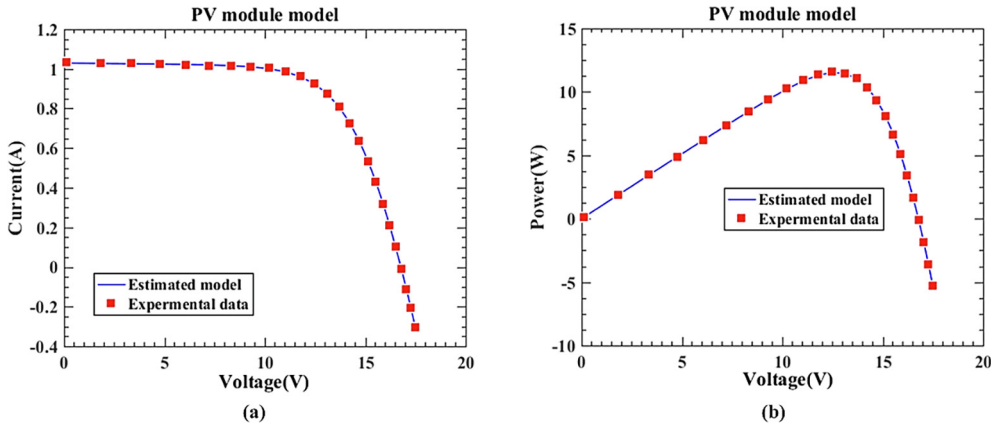

Fig. 11. Comparisons between the experimental and simulated data attained by ISCA for PV module (SDM) (a) I–V characteristics; (b) P–V characteristics.

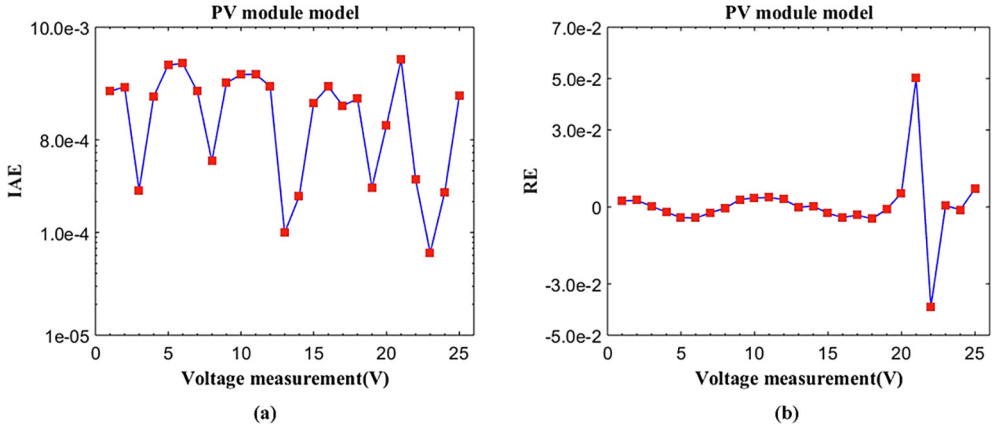

Fig. 12. Error index values of the simulated and the experimental current data of PV module (SDM) (a) IAE values; (b) RE values.

performance of the proposed methods can be accurately evaluated on account of SM55 and ST40. The implemented trial data are carefully extracted from the reference data sheet at different intensities of temperature and irradiation. The attained parameters of SDM and DDM for two PV modules at diverse levels of irradiation and temperature of 25 °C are exhibited in Tables 11 and 12, respectively. In order to validate the accurateness of the rev revealed parameters, the approximated current is achieved and (I-V) characteristics of the two modules are vividly shown with various irradiation intensities, 400 W/m^2, 600 W/m^2, 800 W/m^2 and 1000 W/m^2, as visualized in Figs. 15 and 16. In addition, the attained parameters for SDM and DDM of two PV modules, at dissimilar degrees of temperature and constant irradiation of 1000 W/m^2, are also exposed in Tables 13 and 14, respectively. The experimental and estimated (I-V) characteristics are depicted in Figs. 17 and 18. In terms of SDM, it can be observed that for both PV modules, the (I-V) curves fulfilled from these estimated parameters are highly fitting to the measured curves, under diverse temperatures and irradiation intensities. From Tables 13 and 14, a low RMSE value is attained and generally, the accurateness of the simulated SDM is increased when the irradiation level is at 400 W/m^2, 600 W/m^2, and 800 W/m^2. However, the accuracy is decreased when the irradiation level is 1000 W/m^2. Actually, there are some specific mismatch situations such as partial shading, which may affect the module. Moreover, these parameters are in line with other researches [75]. Regarding the DDM, we see that under different conditions, the estimated results are highly fit to the info ST40 and SM55, even the irradiation levels are low, and a low RMSE value can also be ensured. In short, the competitive and statistical experimental results evidently demonstrated that the proposed ISCA can estimate the appropriate parameters of PV models based under the different temperature and irradiation levels and can work as a promising technique.

Table 8
IAE of ISCA on PV module model.

Item	Measured data		Simulated current data		Simulated power data	
	$V(V)$	$I(A)$	$I_{sim}(A)$	$IAE_I(A)$	$P_{sim}(W)$	$IAE_P(A)$
1	0.1248	1.0315	1.029119083	0.002380917	0.128434062	0.000297138
2	1.8093	1.0300	1.027381020	0.002618980	1.858840480	0.004738520
3	3.3511	1.0260	1.025741767	0.000258233	3.437363235	0.000865365
4	4.7622	1.0220	1.024107146	0.002107146	4.877003050	0.010034650
5	6.0538	1.0180	1.022291815	0.004291815	6.188750189	0.025981789
6	7.2364	1.0155	1.019930709	0.004430709	7.380626582	0.032062382
7	8.3189	1.0140	1.016363150	0.002363150	8.455023408	0.019658808
8	9.3097	1.0100	1.010496210	0.000496210	9.407416565	0.004619565
9	10.2163	1.0035	1.000629040	0.002870960	10.22272646	0.029330586
10	11.0449	0.9880	0.984548457	0.003451543	10.87423926	0.038121943
11	11.8018	0.9630	0.959521758	0.003478242	11.32408389	0.041049511
12	12.4929	0.9255	0.922838898	0.002661102	11.52893406	0.033244886
13	13.1231	0.8725	0.872599733	9.97329E−05	11.45121355	0.001308805
14	13.6983	0.8075	0.807274318	0.000225682	11.05828578	0.003091466
15	14.2221	0.7265	0.728336512	0.001836512	10.35847470	0.026119052
16	14.6995	0.6345	0.637138012	0.002638012	9.365610208	0.038777458
17	15.1346	0.5345	0.536213055	0.001713055	8.115370106	0.025926406
18	15.5311	0.4275	0.429511303	0.002011303	6.670782992	0.031237742
19	15.8929	0.3185	0.318774453	0.000274453	5.066250504	0.004361854
20	16.2229	0.2085	0.207389478	0.001110522	3.364458767	0.018015883
21	16.5241	0.1010	0.096167153	0.004832847	1.589075653	0.079858447
22	16.7987	−0.0080	−0.008325383	0.000325383	−0.139855617	0.005466017
23	17.0499	−0.1110	−0.110936452	6.35481E−05	−1.891455411	0.001083489
24	17.2793	−0.2090	−0.209247200	0.000247200	−3.615645149	0.004271449
25	17.4885	−0.3030	−0.300863480	0.002136520	−5.261650970	0.037364530
Sun of IAE	NA	NA	NA	0.048900000	NA	0.517000000

Table 9
Statistical results of the RMSE values achieved by different algorithms for PV module.

Algorithm	RMSE					
	Min	Median	Mean	Max	SD	Sig
BLPSO	1.30342E−03	1.64321E−03	1.43231E−03	2.19554E−03	2.34234E−04	+
CLPSO	1.23433E−03	1.12343E−03	1.12987E−03	2.34323E−03	3.45633E−04	+
ALCPSO	1.29087E−03	1.13789E−03	2.16543E−03	4.12343E−03	5.54323E−05	+
IJAYA	1.21321E−03	1.43605E−03	1.31245E−03	2.80983E−03	2.45631E−04	+
GOTLBO	1.49087E−03	1.210347E−03	1.21231E−03	2.23109E−03	2.45623E−04	+
ISCA	7.20952E−04	5.36123E−04	6.31252E−04	7.87541E−04	1.67032E−06	

Table 10
Comparison among published different algorithms based on the PV module.

Item	Newton	PS	SA	Method in [73]	COFPANM	ISCA
I_{ph}(A)	1.0318	1.0313	1.0331	1.0339	1.0305143	1.030514201
$I_{sd}(\mu A)$	3.2875	3.1756	3.6642	3.0760	3.4822631	3.4822623
$R_s(\Omega)$	1.2057	1.2053	1.1989	1.2030	1.2012710	1.201271659
$R_{sh}(\Omega)$	555.5556	714.2857	833.3333	555.5556	981.9823286	981.996600
n	48.4500	48.2889	48.8211	48.1862	48.6428351	48.6428300
RMSE	7.8050E−01	1.1800E−02	2.7000E−03	6.1300E−01	2.4250E−03	2.4250E−03

5. Discussion on the results

In this study, two novel effective operators, OBL and NMs, are introduced into original SCA to improve the inclusive exploratory and confined exploitation characteristics of this method and thoroughly investigate the property of ISCA in dealing with the parameter identification of PV model. According to analyzing of competitive experimental results of common solar cell and PV module and two practical datasets from the manufacturers' datasheets, we concede that the proposed framework ISCA can identify the sealed parameters, effectively and efficiently. It also shows superior performance compared to other competitors, which indicates that the balance between the exploration and exploitation trends of the original version is improved to a better extent. With this regard, several reasons can account for the advantage of ISCA that has generated competitive solution on the estimation of the parameters of PV models at different levels of irradiation or temperature.

As it is shown in Section 4, the proposed ISCA was employed to estimate the parameters of photovoltaic models including SDM, DDM and PV cases in Sections 4.1, 4.2 and 4.3, respectively. It can be seen that the ISCA can provide results that are highly in coincidence with all the experimental datasets. The numerical analysis and competitive results including statistical results of the RMSE, evolutionary curves, and parameters achieved by several published methods are vividly reported. As shown in these results, the efficiency of the ISCA was clear according to the mean values and we observed improved evolutionary

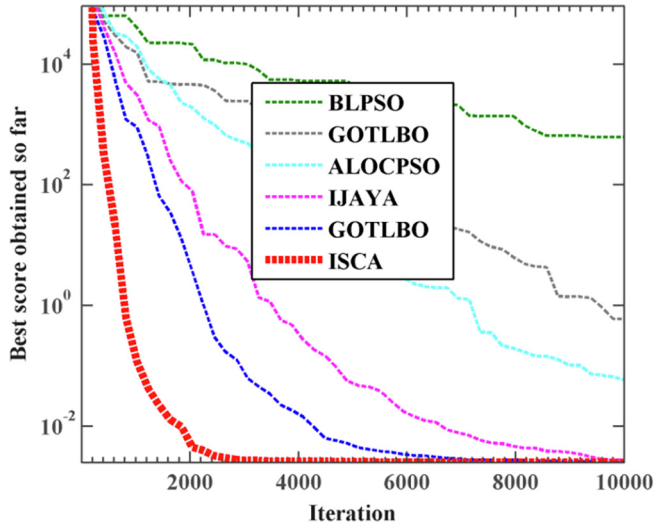

Fig. 13. Convergence graph of different algorithms for the PV module.

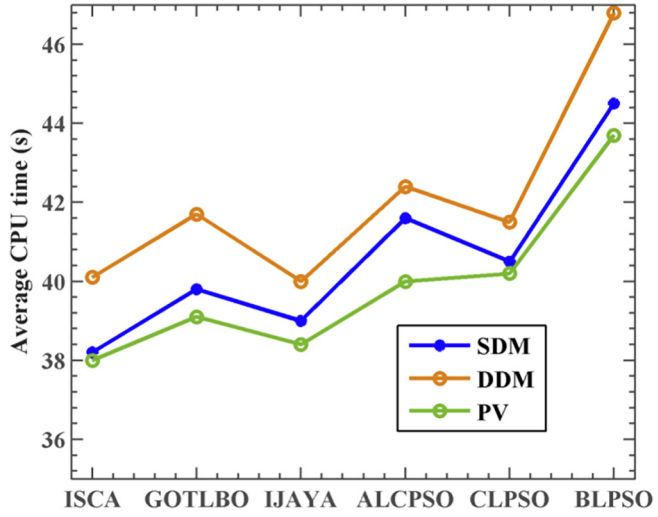

Fig. 14. The average CPU time of different algorithms for RTC France Photowatt-PWP201.

Table 11
Estimated parameters found by the proposed ISCA for three types of PV modules at dissimilar irradiance and temperature of 25 °C based on Thin-film ST40.

Parameters	Irradiance			
	400W/m^2	600W/m^2	800W/m^2	10,000W/m^2
SDM				
I_{Ph}(A)	1.06754448	1.604809857	2.138014468	2.675799241
I_{sd}(μA)	1.8487E−06	1.44198E−06	1.15806E−06	1.52924E−06
R_s(Ω)	1.080582803	1.112595766	1.125287916	1.113206514
R_{sh}(Ω)	362.5082819	347.6905232	332.8905982	357.6151146
n	1.778527063	1.745133834	1.718669231	1.750361233
RMSE	6.3072E−04	6.7404E−04	7.7391E−04	7.3410E−04
DDM				
I_{Ph}(A)	1.067544227	1.604809723	2.138014756	2.675799816
I_{sd1}(μA)	1.84875E−06	1.44187E−06	1.1581E−06	1.5288E−06
I_{sd2}(μA)	2.88658E−19	0	1.16573E−18	2.22045E−20
R_s(Ω)	1.080580319	1.112613741	1.125286813	1.113225983
R_{sh}(Ω)	362.5144985	347.6946879	332.8889434	357.5984399
n_1	1.778530245	1.745124003	1.718673724	1.750326604
n_2	3.77385322	1.031271658	2.677116601	2.383697509
RMSE	6.3072E−04	6.7404E−04	7.7391E−04	7.3410E−04

Table 12
Estimated optimal parameters found by ISCA for three types of PV modules at dissimilar irradiance and temperature of 25 °C based on Mono-crystalline SM55.

Parameters	Irradiance			
	400W/m^2	600W/m^2	800W/m^2	1000W/m^2
SDM				
I_{Ph}(A)	1.382844571	2.070895758	2.760382043	3.450105641
I_{sd}(μA)	1.00421E−07	1.55471E−07	1.43929E−07	1.71149E−07
R_s(Ω)	0.396645384	0.330522568	0.337600394	0.329148924
R_{sh}(Ω)	427.0374184	450.0782568	459.850144	483.868452
n	1.351988922	1.387511003	1.381132696	1.395750438
RMSE	7.0761E−04	8.2395E−04	6.6858E−04	1.1462E−03
DDM				
I_{Ph}(A)	1.382295701	2.070896544	2.760381699	3.450103564
I_{sd1}(μA)	4.93671E−08	4.2466E−18	1.43951E−07	7.38298E−19
I_{sd2}(μA)	1E−04	1.55514E−07	5.88418E−19	1.71154E−07
R_s(Ω)	0.448029925	0.330502518	0.337590229	0.329147704
R_{sh}(Ω)	475.6944577	450.068517	459.8785018	483.9004816
n_1	1.297634572	3.279006274	1.381144518	3.722694119
n_2	4	1.387534223	3.497711021	1.395752862
RMSE	5.9929E−04	8.2395E−04	6.6858E−04	1.1462E−03

convergence behaviors compared to other peers. Convergence curves reveal the accelerated trends of the ISCA, which is mainly due to the diversification potentials of the OBL-based operator. A main reason for the improvements is that the OBL-based exploration phases and NMs-based exploitation strategies can uphold a more stable, reasonable equilibrium between the diversification and intensification proclivities. Furthermore, the NMs can perform an iterative exploitation stage in neighborhoods of better solutions, which will lead to enhancement in the local search abilities of the SCA. It can guarantee more effective exploitation in the case of finding a high-quality solution. Therefore, the ISCA has an effective local search capability compared to the conventional method. Note that the scatter patterns of OBL-based phase in ISCA positively enhance the diversity of solutions to explore different regions of feature space. In ISCA, the opposite solutions are considered, which guarantee the higher chance of this method in escaping from the local optima and stagnation problems.

Furthermore, two practical datasets obtained from the manufacturers' dataset including ST40 and SM55 were both utilized to thoroughly investigate the performance of the proposed ISCA for this complex task at different levels of temperature and irradiation. It can be observed that the estimated parameters can still be highly matched with the practical data ST40 and SM55, even being in the low-temperature condition, and an ideal low RMSE value can also be guaranteed, which indicates that stability of the SCA has been improved, significantly. This is due to a more stable tradeoff between the core searching leanings of the proposed ISCA and its enriched algorithmic structure. This indicates that the OBL-based ISCA can be a more effective optimizer for these tasks. Based on the discussion above, it is understood that the behaviors of the original SCA for the estimation of PV parameters have been enhanced because of the introduced NM and OBL-based operators, significantly. Therefore, in the practical cases, the ISCA can be regarded as an auxiliary and effective alternative technique to estimate the parameters of the solar cell panels.

Please note that ISCA cannot be considered as a universal best method based on no free lunch (NFL) theorem [47]. Based on NFL, such a method does not exist and ISCA is not an exception. In addition, ISCA is still a population-based optimizer with randomized components. Hence, it may still face stagnation problems and immature convergence in dealing with some harder datasets.

6. Conclusion and future directions

In this paper, an enhanced SCA is designed to identify the unknown

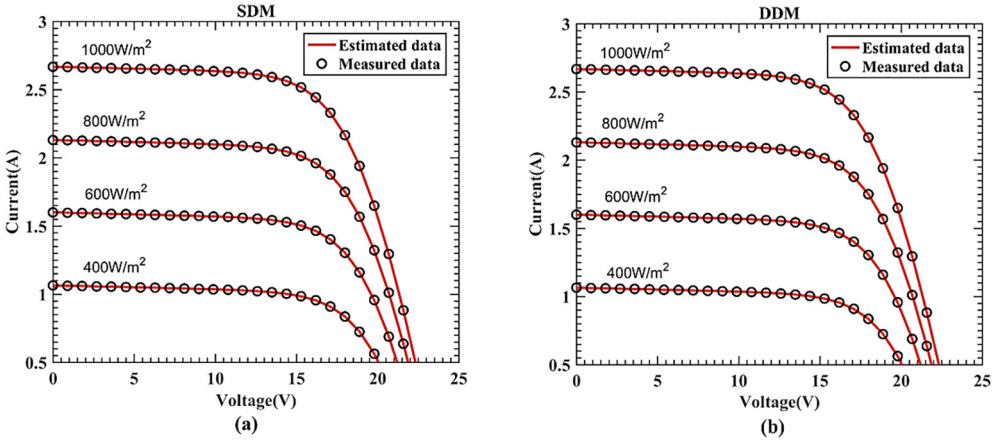

Fig. 15. Estimated and measured (I-V) characteristics for Thin-film ST40 at diverse irradiance for both SDM and DDM.

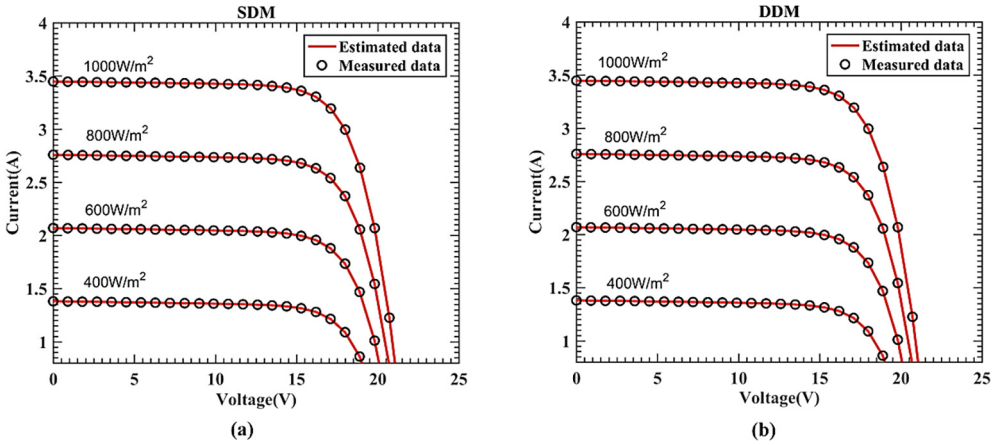

Fig. 16. Estimated and measured (I-V) characteristics for Mono-crystalline SM55 at diverse irradiance for both SDM and DDM.

Table 13
The optimal extracted parameters for Thin-film ST40 PV module found by ISCA at diverse temperatures and irradiance of 1000 W/m^2.

Parameters	Temperature			
	25 °C	40 °C	50 °C	70 °C
SDM				
I_{Ph}(A)	2.67580148	2.680913523	2.691970413	2.692329657
I_{sd}(μA)	1.52866E−06	5.66547E−06	1.86789E−05	8.75205E−05
R_s(Ω)	1.11323541	1.129306396	1.149596752	1.125890161
R_{sh}(Ω)	357.585963	364.0897367	295.0004305	367.7481449
n	1.75031577	1.72254314	1.717562053	1.727317377
RMSE	7.3410E−04	1.3214E−03	1.8233E−03	7.7772E−04
DDM				
I_{Ph}(A)	2.675799817	2.680911957	2.690053785	2.692329477
I_{sd1}(μA)	3.47007E−14	5.6661E−06	3.10638E−05	1.36169E−17
I_{sd2}(μA)	1.5288E−06	2.46136E−17	1.69254E−09	8.75219E−05
R_s(Ω)	1.113225987	1.129297714	1.2541736	1.125888711
R_{sh}(Ω)	357.5984382	364.1097321	350.1287327	367.7532324
n_1	1.750354824	1.722557644	1.852757101	2.273800412
n_2	1.750326599	3.999928999	1.020121776	1.727319867
RMSE	7.3410E−04	1.3214E−03	1.5514E−03	7.7772E−04

Table 14
The optimal extracted parameters for Mono-crystalline SM55 PV module found by the ISCA at diverse temperatures and irradiance of 1000 W/m^2.

Parameters	Temperature		
	25 °C	40 °C	60 °C
SDM			
I_{Ph}(A)	3.450103977	3.469136617	3.494608701
I_{sd}(μA)	1.71162E−07	1.14513E−06	6.9095E−06
R_s(Ω)	0.329145446	0.313096133	0.318706126
R_{sh}(Ω)	483.895421	533.1160342	484.8759188
n	1.395756915	1.417841102	1.405141802
RMSE	1.1462E−03	3.7888E−03	3.7804E−03
DDM			
I_{Ph}(A)	3.450103564	3.469137516	3.49460847
I_{sd1}(μA)	1.71154E−07	2.55851E−17	1.45994E−18
I_{sd2}(μA)	9.12603E−18	1.14511E−06	6.9095E−06
R_s(Ω)	0.329147705	0.313095936	0.318705731
R_{sh}(Ω)	483.9004773	533.0691776	484.883911
n_1	1.395752859	3.916252155	3.998744211
n_2	3.940098455	1.417839751	1.405141742
RMSE	1.1462E−03	3.7888E−03	3.7804E−03

parameters of solar cell models and photovoltaic models, accurately and efficiently. In the ISCA, a framework is proposed by integrating the SCA with NMs-based exploitation strategy and OBL-based diversification mechanism. ISCA utilizes the cores of sine cosine algorithm along with the Nelder-Mead simplex to exploit the locality of high-quality agents; meanwhile, it employs opposition-based learning to explore the search space, effectively. Hence, the ISCA is able to obtain a more stable tradeoff between the intensification and diversification tendencies. This balance is significantly beneficial in alleviating the immature convergence and stagnation drawbacks. In addition, it boosts the quality of solutions. We can conclude that the proposed ISCA framework is a potential technique in the identification of parameters of these models.

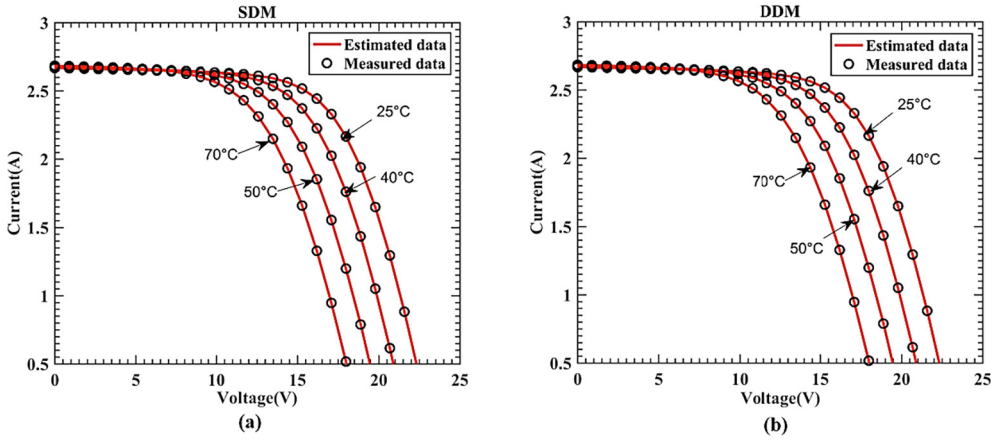

Fig. 17. Estimated and measured (I-V) characteristics for Thin-film ST40 at diverse temperatures for SDM and DDM.

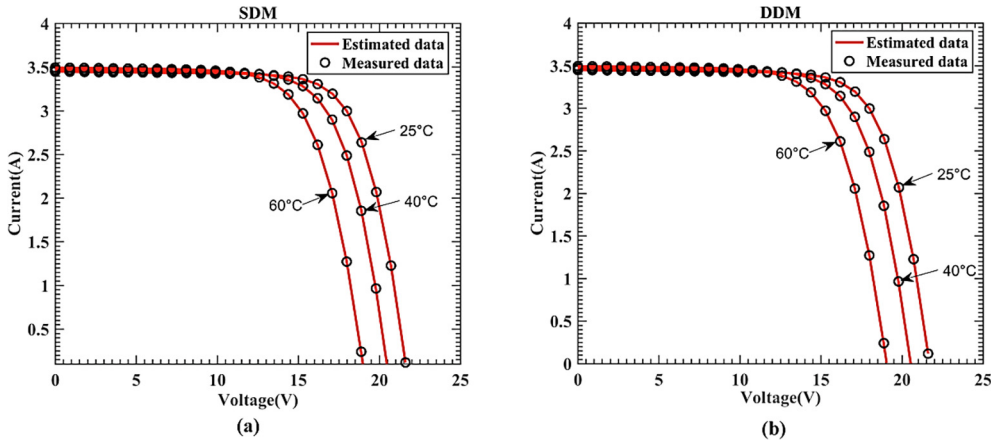

Fig. 18. Estimated and measured (I-V) characteristics for Mono-crystalline SM55 at different temperatures for SDM and DDM.

Regarding the competitive and statistical experimental results, the following conclusions can be made:

I. The evolution curves indicate that ISCA has a very fast convergence speed compared to other competitors.
II. According to the experimental results, ISCA exhibits a superior and very competitive performance compared with several well-established algorithms such as the CPSO, PS, ABC, ABSO, GOTLBO, SA, and GOFPANM in dealing with different PV parameters estimation problems.
III. Based on testing at different levels of temperature and irradiation, ISCA also maintains a more stable efficacy.
IV. Evaluations and results indicate that this proposal can be treated as a new potential and promising technique for parameters estimation of different solar cells and PV models.

Although competitive analysis has demonstrated the efficiency of the proposed methodology for PV parameters estimation, there are still some limited aspects that can be further explored in future works. First, the proposed ISCA can be employed into other solar cell models based on various practical datasets to exert its capability thoroughly. Mainly, it is interesting to consider the unstable environmental factors such as wind, rain and so on in designing experimental details. Secondly, the performance of the proposed ISCA can be further improved based on other optimization methods and paradigms. Please note that ISCA cannot be considered as a universal best method because such a method does not exist, as a statement of NFL theorem. In addition, ISCA is a stochastic population-based optimizer. Hence, it may still face stagnation problems in dealing with some harder datasets. In addition, the proposed method cannot deal with multi-objective problems. Hence, the multi-objective variant of the ISCA will also be developed and studied.

Declaration of Competing Interest

The authors declare that there is no conflict of interests regarding the publication of article.

Acknowledgments

This research is supported by the Natural Science Foundation of Zhejiang Province, China (LY17F020012), Wenzhou Municipal Science and Technology Bureau (ZG2017019), Natural Science Foundation of Guangdong Province (2018A030313339), Humanities and Social Science Fund of Ministry of Education of China (17YJCZH261), National Natural Science Foundation of China (61471133, 61871475) and Science and Technology Planning Project of Shenzhen Municipality (JCYJ20170303094658400).

References

[1] Alhajri MF, El-Naggar KM, Alrashidi MR, Al-Othman AK. Optimal extraction of solar cell parameters using pattern search. Renew Energy 2012;44:238–45.
[2] Nassar-Eddine I, Obbadi A, Errami Y, Fajri AE, Agunaou M. Parameter estimation of photovoltaic modules using iterative method and the Lambert W function: a comparative study. Energy Convers Manage 2016;119:37–48.
[3] Parida B, Iniyan S, Goic R. A review of solar photovoltaic technologies. Renew Sustain Energy Rev 2011;15:1625–36.
[4] Chen Z, Wu L, Lin P, Wu Y, Cheng S, Yan J. Parameters identification of photovoltaic models using hybrid adaptive Nelder-Mead simplex algorithm based on

eagle strategy. Appl Energy 2016;182:47–57.
[5] Fathy A, Rezk H. Parameter estimation of photovoltaic system using imperialist competitive algorithm. Renew Energy 2017;111.
[6] Jordehi AR. Enhanced leader particle swarm optimisation (ELPSO): an efficient algorithm for parameter estimation of photovoltaic (PV) cells and modules. Sol Energy 2018;159:78–87.
[7] Oliva D, Aziz MAE, Hassanien AE. Parameter estimation of photovoltaic cells using an improved chaotic whale optimization algorithm. Appl Energy 2017;200:141–54.
[8] Das UK, Tey KS, Idris MYI, Mekhilef S, Seyedmahmoudian M, Horan B, et al. Forecasting of photovoltaic power generation and model optimization. Renew Sustain Energy Rev 2018;81.
[9] Alam DF, Yousri DA, Eteiba MB. Flower pollination algorithm based solar PV parameter estimation. Energy Convers Manage 2015;101:410–22.
[10] Humada AM, Hojabri M, Mekhilef S, Hamada HM. Solar cell parameters extraction based on single and double-diode models: a review. Renew Sustain Energy Rev 2016;56:494–509.
[11] Ma J, Ting TO, Man KL, Zhang N, Guan SU, Wong PWH. Parameter estimation of photovoltaic models via cuckoo search. J Appl Math 2013:1–11.
[12] Gao W, Guirao JLG, Abdel-Aty M, Xi W. An independent set degree condition for fractional critical deleted graphs. Discrete Continuous Dyn Syst-Series S 2019;12:877–86.
[13] Gao W, Wang W, Dimitrov D, Wang Y. Nano properties analysis via fourth multiplicative ABC indicator calculating. Arab J Chem 2018;11:793–801.
[14] Wei G, Darko D, Hosam A. Tight independent set neighborhood union condition for fractional critical deleted graphs and ID deleted graphs. Discrete Continuous Dyn Syst – S 2018;12:711–21.
[15] Gao W, Guirao JLG, Basavanagoud B, Wu J. Partial multi-dividing ontology learning algorithm. Inf Sci 2018;467:35–58.
[16] Gao W, Wu H, Siddiqui MK, Baig AQ. Study of biological networks using graph theory. Saudi J Biol Sci 2018;25:1212–9.
[17] Niu Q, Zhang H, Li K. An improved TLBO with elite strategy for parameters identification of PEM fuel cell and solar cell models. Int J Hydrogen Energy 2014;39:3837–54.
[18] Yu K, Chen X, Wang X, Wang Z. Parameters identification of photovoltaic models using self-adaptive teaching-learning-based optimization. Energy Convers Manage 2017;145:233–46.
[19] Chan DSH, Phillips JR, Phang JCH. A comparative study of extraction methods for solar cell model parameters. Solid State Electron 1986;29:329–37.
[20] Easwarakhanthan T, Bottin J, Bouhouch I, Boutrit C. Nonlinear minimization algorithm for determining the solar cell parameters with microcomputers. Int J Solar Energy 1986;4:1–12.
[21] Aljarah I, Mafarja M, Heidari AA, Faris H, Zhang Y, Mirjalili S. Asynchronous accelerating multi-leader salp chains for feature selection. Appl Soft Comput 2018;71:964–79.
[22] Heidari AA, Aljarah I, Faris H, Chen H, Luo J, Mirjalili S. An enhanced associative learning-based exploratory whale optimizer for global optimization. Neural Comput Appl 2019.
[23] Mafarja M, Aljarah I, Heidari AA, Faris H, Fournier-Viger P, Li X, et al. Binary dragonfly optimization for feature selection using time-varying transfer functions. Knowl-Based Syst 2018;161:185–204.
[24] Zhang Q, Chen H, Heidari AA, Zhao X, Xu Y, Wang P, et al. Chaos-induced and mutation-driven schemes boosting salp chains-inspired optimizers. IEEE Access 2019;7:31243–61.
[25] Heidari AA, Mirjalili S, Faris H, Aljarah I, Mafarja M, Chen H. Harris hawks optimization: algorithm and applications. Future Generation Comput Syst 2019;97:849–72.
[26] Chen H, Xu Y, Wang M, Zhao X. A balanced whale optimization algorithm for constrained engineering design problems. Appl Math Model 2019;71:45–59.
[27] Deng W, Xu J, Zhao H. An improved ant colony optimization algorithm based on hybrid strategies for scheduling problem. IEEE Access 2019;7:20281–92.
[28] Deng W, Zhao H, Yang X, Xiong J, Sun M, Li B. Study on an improved adaptive PSO algorithm for solving multi-objective gate assignment. Appl Soft Comput J 2017;59:288–302.
[29] Ishaque K, Salam Z, Mekhilef S, Shamsudin A. Parameter extraction of solar photovoltaic modules using penalty-based differential evolution. Appl Energy 2012;99:297–308.
[30] Jiang LL, Maskell DL, Patra JC. Parameter estimation of solar cells and modules using an improved adaptive differential evolution algorithm. Appl Energy 2013;112:185–93.
[31] Huang W, Jiang C, Xue L, Song D. Extracting solar cell model parameters based on chaos particle swarm algorithm. International conference on electric information and control engineering. 2011. p. 398–402.
[32] El-Naggar KM, Alrashidi MR, Alhajri MF, Al-Othman AK. Simulated Annealing algorithm for photovoltaic parameters identification. Sol Energy 2012;86:266–74.
[33] Dkhichi F, Oukarfi B, Fakkar A, Belbounaguia N. Parameter identification of solar cell model using Levenberg–Marquardt algorithm combined with simulated annealing. Sol Energy 2014;110:781–8.
[34] Rajasekar N, Kumar NK, Venugopalan R. Bacterial Foraging Algorithm based solar PV parameter estimation. Sol Energy 2013;97:255–65.
[35] Oliva D, Cuevas E, Pajares G. Parameter identification of solar cells using artificial bee colony optimization. Energy 2014;72:93–102.
[36] Askarzadeh A, Rezazadeh A. Artificial bee swarm optimization algorithm for parameters identification of solar cell models. Appl Energy 2013;102:943–9.
[37] Askarzadeh A, Rezazadeh A. Parameter identification for solar cell models using harmony search-based algorithms. Sol Energy 2012;86:3241–9.
[38] Allam D, Yousri DA, Eteiba MB. Parameters extraction of the three diode model for the multi-crystalline solar cell/module using Moth-Flame Optimization Algorithm. Energy Convers Manage 2016;123:535–48.
[39] Awadallah MA. Variations of the bacterial foraging algorithm for the extraction of PV module parameters from nameplate data. Energy Convers Manage 2016;113:312–20.
[40] Xu S, Wang Y. Parameter estimation of photovoltaic modules using a hybrid flower pollination algorithm. Energy Convers Manage 2017;144:53–68.
[41] Nunes HGG, Pombo JAN, Bento PMR, Mariano SJPS, Calado MRA. Collaborative swarm intelligence to estimate PV parameters. Energy Convers Manage 2019;185:866–90.
[42] Abbassi R, Abbassi A, Heidari AA, Mirjalili S. An efficient salp swarm-inspired algorithm for parameters identification of photovoltaic cell models. Energy Convers Manage 2019;179:362–72.
[43] Yousri D, Allam D, Eteiba MB, Suganthan PN. Static and dynamic photovoltaic models' parameters identification using Chaotic Heterogeneous Comprehensive Learning Particle Swarm Optimizer variants. Energy Convers Manage 2019;546–63.
[44] Aljarah I, Mafarja M, Heidari AA, Faris H, Mirjalili S. Clustering analysis using a novel locality-informed grey wolf-inspired clustering approach. Knowl Inf Syst 2019.
[45] Faris H, Ala'M A-Z, Heidari AA, Aljarah I, Mafarja M, Hassonah MA, et al. An intelligent system for spam detection and identification of the most relevant features based on evolutionary Random Weight Networks. Inf Fusion 2019;48:67–83.
[46] Faris H, Mafarja MM, Heidari AA, Aljarah I, Ala'M A-Z, Mirjalili S, et al. An efficient binary Salp Swarm Algorithm with crossover scheme for feature selection problems. Knowl-Based Syst 2018;154:43–67.
[47] Wolpert DH, Macready WG. No free lunch theorems for optimization. IEEE Trans Evol Comput 1997;1:67–82.
[48] Mafarja M, Aljarah I, Heidari AA, Hammouri AI, Faris H, Ala'M A-Z, et al. Evolutionary population dynamics and grasshopper optimization approaches for feature selection problems. Knowl-Based Syst 2018;145:25–45.
[49] Luo J, Chen H, Heidari AA, Xu Y, Zhang Q, Li C. Multi-strategy boosted mutative whale-inspired optimization approaches. Appl Math Model 2019;73:109–23.
[50] Mirjalili S. SCA: a sine cosine algorithm for solving optimization problems. Knowl-Based Syst 2016;96:120–33.
[51] Nenavath H, Jatoth DRK, Das DS. A synergy of the sine-cosine algorithm and particle swarm optimizer for improved global optimization and object tracking. Swarm Evol Comput 2018.
[52] Hafez AI, Zawbaa HM, Emary E, Hassanien AE. Sine cosine optimization algorithm for feature selection. International symposium on innovations in intelligent systems and applications. 2016.
[53] Bairathi D, Gopalani D. Opposition-Based Sine Cosine Algorithm (OSCA) for Training Feed-Forward Neural Networks. International conference on signal-image technology & internet-based systems. 2017. p. 438–44.
[54] Sahlol AT, Ewees AA, Hemdan AM, Hassanien AE. Training feedforward neural networks using Sine-Cosine algorithm to improve the prediction of liver enzymes on fish farmed on nano-selenite. Computer engineering conference. 2017.
[55] Das S, Bhattacharya A, Chakraborty AK. Solution of short-term hydrothermal scheduling using sine cosine algorithm. Soft Comput 2017;1–19.
[56] Tawhid MA, Savsani V. Multi-objective sine-cosine algorithm (MO-SCA) for multi-objective engineering design problems. Neural Comput Appl 2017:1–15.
[57] Issa M, Hassanien AE, Oliva D, Helmi A, Ziedan I, Alzohairy A. ASCA-PSO: adaptive sine cosine optimization algorithm integrated with particle swarm for pairwise local sequence alignment. Expert Syst Appl 2018;99:56–70.
[58] Xu Y, Chen H, Heidari AA, Luo J, Zhang Q, Zhao X, et al. An efficient chaotic mutative moth-flame-inspired optimizer for global optimization tasks. Expert Syst Appl 2019.
[59] Xu C, Tianfield H, Mei C, Du W, Liu G. Biogeography-based learning particle swarm optimization. Soft Comput 2016;21:1–23.
[60] Liang JJ, Qin AK, Suganthan PN, Baskar S. Comprehensive learning particle swarm optimizer for global optimization of multimodal functions. IEEE Trans Evol Comput 2006;10:281–95.
[61] Chen WN, Zhang J, Lin Y, Chen N, Zhan ZH, Chung SH, et al. Particle swarm optimization with an aging leader and challengers. IEEE Trans Evol Comput 2013;17:241–58.
[62] Yu K, Liang JJ, Qu BY, Xu C, Wang H. Parameters identification of photovoltaic models using an improved JAYA optimization algorithm. Energy Convers Manage 2017;150:742–53.
[63] Xu C, Yu K, Du W, Zhao W, Liu G. Parameters identification of solar cell models using generalized oppositional teaching learning based optimization. Energy 2016;99:170–80.
[64] Chen X, Yu K, Du W, Zhao W, Liu G. Parameters identification of solar cell models using generalized oppositional teaching learning based optimization. Energy 2016;99:170–80.
[65] Gao XK, Cui Y, Hu JJ, Xu GY, Wang ZF, Qu JH, et al. Parameter extraction of solar cell models using improved shuffled complex evolution algorithm. Energy Convers Manage 2018;157:460–79.
[66] Nelder JA, Mead R. A simplex method for function minimization. Comput J 1965;7:308–13.
[67] Fan SKS, Zahara E. A hybrid simplex search and particle swarm optimization for unconstrained optimization. Eur J Oper Res 2007;181:527–48.
[68] Masoudipour N, Hadizadeh M. Application of the genetic algorithm and downhill simplex methods (Nelder–Mead methods) in the search for the optimum chiller configuration. Appl Therm Eng 2013;61:433–42.
[69] Tizhoosh HR. Opposition-based learning: A new scheme for machine intelligence. Computational intelligence for modelling, control and automation. 2005 and international conference on intelligent agents, web technologies and internet

commerce, international conference. 2005. p. 695–701.
[70] Ventresca M, Tizhoosh HR. Opposite transfer functions and backpropagation through time. Foundations of computational intelligence, 2007 FOCI 2007 IEEE Symposium. 2007. p. 570–7.
[71] Ventresca M, Tizhoosh HR. Simulated annealing with opposite neighbors. Foundations of computational intelligence, 2007 FOCI 2007 IEEE symposium. 2007. p. 186–92.
[72] Tizhoosh HR, Sahba F. Quasi-global oppositional fuzzy thresholding. IEEE international conference on fuzzy systems, 2009 Fuzz-IEEE. 2009. p. 1346–51.
[73] Bouzidi K, Chegaar M, Nehaoua N. New methods to extract the parameters of solar cells from their illuminated I-V Curve Algeria 4th international conference on computer integrated manufacturing Setif. 2007.
[74] Shell st40 photovoltaic solar module. URL < http://www.aeet-service.com/pdf/shell/Shell-Solar_ST40.pdf > .
[75] Shell sm55 photovoltaic solar module. URL < http://www.aeet-service.com/pdf/shell/Shell-Solar_SM55.pdf > .
[76] Yu K, Qu B, Yue C, Ge S, Chen X, Liang J. A performance-guided JAYA algorithm for parameters identification of photovoltaic cell and module. Appl Energy 2019;237:241–57.